

EPITAXIAL GROWTH OF HIGH CURIE-TEMPERATURE $\text{Ge}_{1-x}\text{Mn}_x$ QUANTUM DOTS ON Si(001) BY SELF-ASSEMBLY

LUONG THI KIM PHUONG

*Aix Marseille University, CNRS, CINaM-UMR 7325, F-13288 Marseille, France
and*

Hong Duc University, 565 Quang Trung St., Thanh Hoa City, Vietnam

NGUYEN MANH AN

Hong Duc University, 565 Quang Trung St., Thanh Hoa City, Vietnam

E-mail:

Received 25 September 2013

Accepted for publication 22 October 2013

Abstract. *We report on successful growth of epitaxial high Curie-temperature $\text{Ge}_{1-x}\text{Mn}_x$ quantum dots on Si (001) substrates using the self-assembled approach. By decreasing the growth temperature down to 400 °C, we show that the Mn diffusion into the Si substrate can be neglected. No indication of secondary phases or clusters was observed. $\text{Ge}_{1-x}\text{Mn}_x$ quantum dots were found to be epitaxial and perfectly coherent to the Si substrate. We also evidence that the ferromagnetic ordering in $\text{Ge}_{1-x}\text{Mn}_x$ quantum dots persists up to a temperature higher 320 K. It is believed that single-crystalline quantum dots exhibiting a high Curie temperature are potential candidates for the realization of nanoscale spintronic devices.*

Keywords: *ferromagnetic quantum dots, self-assembly, high Curie temperature, spintronics, Stranski-Krastanov growth.*

I. INTRODUCTION

As the device miniaturization reaches technological and physical limits, adding the spin degree of freedom to the electron into conventional electronics appears as a promising solution for the development of a new generation of devices [1]. The development of such spin-based devices requires an efficient injection of spin-polarized currents from ferromagnetic materials into conventional semiconductors. Research dealing with group-IV semiconductors, such as silicon and germanium, represents a particular interest since it allows integrating spintronic devices into the existing Si technology. Germanium, thanks to its small band gap and its high mobility, is believed to lead to a new generation of devices, exhibiting high-speed data processing, high-density integration and low power consumption [2] In addition, its long spincoherence time is of great advantage for innovative spintronic devices.

To develop spintronic devices, one of the key requirements is to obtain adequate spin injectors, which should have not only a high Curie temperature (T_C) and a high spin polarization but also are compatible with the existing Si complementary metal-oxide semiconductor (CMOS)

technology. Silicon- or germanium-based diluted ferromagnetic semiconductors (DMS) would be ideal candidates since they exhibit a natural impedance match to group-IV semiconductors. Unfortunately, $\text{Si}_{1-x}\text{Mn}_x$ alloys are not ferromagnetic and the use of $\text{Ge}_{1-x}\text{Mn}_x$ alloys for the device fabrication has been largely hampered by their low Curie temperature [3]. Indeed, since the first paper of Park *et al.* published in 2002 [3], which reported the existence of ferromagnetism up to 116 K in $\text{Ge}_{1-x}\text{Mn}_x$ thin films, these materials have attracted much attention [4-12]. However, in spite of more than 10 years of intense research, it has not been demonstrated in a reproducible manner that the Curie temperature of $\text{Ge}_{1-x}\text{Mn}_x$ thin films could exceed 150 K. Such a low Curie temperature is mainly attributed to a low solubility of magnetic elements in semiconductors, which above a few % leads to the formation of highly inhomogeneous materials. It is indeed now generally accepted that the Mn_5Ge_3 compound is likely to be formed, as precipitates, during the growth process of $\text{Ge}_{1-x}\text{Mn}_x$ diluted magnetic semiconductors [13-18].

To get spin injectors of higher Curie temperatures, alternative approaches, such as the use of epitaxial high- T_C Mn_5Ge_3 and carbon-doped $\text{Mn}_5\text{Ge}_3\text{C}_x$ compounds, have been developed [19-27]. However, since these compounds are intermetallic, they form a Schottky barrier at the interface with Ge, which may limit the efficiency of spin injection.

In this work, we investigate the epitaxial growth and the magnetic property of Mn-doped Ge quantum dots (QDs). If it will be possible to produce diluted magnetic $\text{Ge}_{1-x}\text{Mn}_x$ QDs, which exhibit a Curie temperature higher than room temperature while conserving their semiconducting properties, those quantum dots would become an ideal candidate for spin injection into group-IV semiconductors. Here, we implement the growth of $\text{Ge}_{1-x}\text{Mn}_x$ quantum dots on a silicon substrate using the self-assembled technique, which is based on the strain-driven growth mode transition from two-dimensional growth to the formation of islands in a high lattice mismatched system (Stranski-Krastanov growth) [28, 29]. We have combined structural and magnetic characterizations to study the $\text{Ge}_{1-x}\text{Mn}_x$ QD size, density and their magnetic properties. We show that $\text{Ge}_{1-x}\text{Mn}_x$ QDs can be epitaxially grown on a Si(001) substrate without any formation of Mn clusters or secondary phases. Of the most important, we provide evidence that $\text{Ge}_{1-x}\text{Mn}_x$ QDs display ferromagnetic ordering well above room temperature.

II. EXPERIMENTAL SET-UP

$\text{Ge}_{1-x}\text{Mn}_x$ quantum dots were grown on Si(001) substrates using co-deposition of Mn and Ge in a molecular-beam epitaxial (MBE) system with a base pressure better than 3×10^{10} mbar. The Mn concentration (x) was chosen to be of about 2 % in order to produce diluted magnetic QDs and to conserve their semiconducting properties. The Si(001) substrate surface was cleaned in solvents and then etched with numerous cycles in HF/hot HNO_3 solutions to remove the contaminated surface region and native silicon dioxide (SiO_2). Finally, before introduction of the sample into high vacuum, a very thin oxide layer was chemically formed in a $\text{HCl}:\text{H}_2\text{O}_2:\text{H}_2\text{O}$ (3:1:1) solution to protect the Si surface against oxidation in ambient air. *In-situ* thermal cleaning was carried out in the MBE chamber at 900 °C to remove this oxide film, which gives rise to the formation of a (2x1) reconstructed Si surface. The Mn and Ge concentrations were pre-estimated by flux measurements using a quartz crystal microbalance and confirmed by energy dispersive X-ray spectroscopy measurements (EDX). Reflection high-energy electron diffraction (RHEED) was used to probe the surface reconstruction and the change of the growth mode during $\text{Ge}_{1-x}\text{Mn}_x$ deposition. The RHEED technique was operated with a 30 keV electron beam at an incidence angle of about

1°. The surface morphology of QDs was analysed by atomic force microscopy (AFM) in contact mode at room temperature. A JEOL high-resolution transmission electron microscope (HR-TEM) operating at 300 kV was used to investigate the cross-sectional structure of the samples. Finally, the magnetic properties were determined using a combined vibrating sample magnetometer with superconducting quantum interference device magnetometer (VSM-SQUID) from Quantum Designs which provide a sensitivity of about 100 times higher than that of a standard SQUID. The diamagnetic contribution of the Si substrate was subtracted from the measurements, leaving the magnetic signal of $\text{Ge}_{1-x}\text{Mn}_x$ QDs.

III. RESULTS AND DISCUSSION

It is now generally accepted that because the lattice parameter of pure Ge (0.465 nm) is about 4,2 % larger than that of Si (0.453 nm), the growth of Ge on Si proceeds via the Stranski-Krastanov mode, *i.e.* a layer-by-layer (2D) growth mode for film thicknesses below a critical thickness (h_c), which is about 4-6 atomic planes, beyond which a transition to a three-dimensional (3D) island growth mode occurs [30-32]. From thermodynamic considerations, the island formation is energetically favorable because the energy, which is gained from a *partial* strain relaxation of islands, is large enough to outweigh the increase of the surface energy due to the increase of the surface area. Thus, the driving force for the Ge/Si growth mode transition from 2D to 3D growth when the film thickness increases is to minimize the total energy of the system. Of particular interest, in the early stage of their formation, the islands can have a small size and are perfectly coherent to the substrate lattice [28].

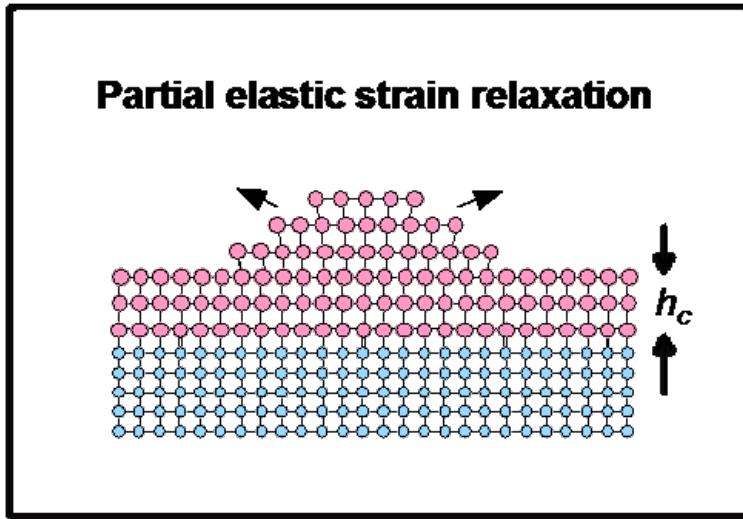


Fig. 1. Schema illustrating the Stranski-Krastanov growth of self-assembled Ge quantum dots on Si. When the deposited Ge thickness becomes larger than h_c , islands are formed on the top of the wetting layer.

Shown in Fig. 1 is a schema illustrating the Stranski-Krastanov growth of Ge on Si. When the Ge deposited thickness is smaller than the critical thickness, the Ge growth is two-dimensional (formation of the wetting layer) and the Ge film is laterally compressed. For the Ge thickness larger than the critical thickness, 3D islands are formed on the top of the two-dimensional wetting layer. It is worth noting that 3D islands are partially relaxed but they are free of dislocations and remain perfectly coherent to the substrate.

The RHEED technique, thanks to its grazing incidence, can be extremely sensitive to the morphology of the growing surface. When the growth is 2D, RHEED patterns consist of long streaks due to *reflection* diffraction on a smooth surface. With the appearance of 3D islands, RHEED is characterized by spotty patterns due to *transmission* diffraction across the islands. It is worth noting that when the Ge layer is doped with a Mn concentration of about 2 %, the misfit between the $\text{Ge}_{0.98}\text{Mn}_{0.02}$ alloy and the Si substrate is only slightly reduced as compared to that of pure Ge on Si. This implies that the Stranski-Krastanov growth of the $\text{Ge}_{0.98}\text{Mn}_{0.02}$ alloy should be maintained. Figure 2(a) displays a RHEED pattern taken along the [110] azimuth after deposition of about 1.2 nm thick $\text{Ge}_{0.98}\text{Mn}_{0.02}$ films on Si(001). As expected, we observe here a 3D spotty pattern, indicating that $\text{Ge}_{0.98}\text{Mn}_{0.02}$ islands have been effectively formed on the surface. In addition, 3D spots are arranged along a two-fold symmetry, similar that of the [001] plane of the Ge or Si. This implies that $\text{Ge}_{0.98}\text{Mn}_{0.02}$ islands are formed with their (001) planes being parallel to the (001) plane of the Si substrate. In other words, $\text{Ge}_{0.98}\text{Mn}_{0.02}$ islands are epitaxially grown on the Si(001) substrate.

It is worth noting that in the whole growth temperature range, going from 400 to 650 °C, we observe the same RHEED patterns during the growth of the $\text{Ge}_{0.98}\text{Mn}_{0.02}$ alloy. However, it is important to recall that in the case of pure Ge on Si, it has been demonstrated that Ge islands are not pure but formed by a SiGe alloy [33] and the Si concentration inside Ge islands has been found to increase with increasing the growth temperature [30, 34]. Since in the bulk phase diagram, Mn-doped Si alloys are not ferromagnetic, therefore in order to have a chance to produce high Curie-temperature $\text{Ge}_{1-x}\text{Mn}_x$ quantum dots, it is of great importance to reduce as much as possible the degree of Si/Ge interdiffusion during the formation of $\text{Ge}_{1-x}\text{Mn}_x$ QDs. We have then investigated the growth of the $\text{Ge}_{0.98}\text{Mn}_{0.02}$ alloy on Si at various substrate temperatures and found that the lowest temperature at which $\text{Ge}_{0.98}\text{Mn}_{0.02}$ islands could be formed is at 400 °C. Below this temperature a pseudo two-dimensional and metastable film is formed [35]. We also note that to date there have been only two papers reporting the growth of $\text{Ge}_{1-x}\text{Mn}_x$ quantum dots [36, 37] and in both papers the growth temperature is 450 °C. Figure 2(b) displays an AFM image of a 1.2 nm thick $\text{Ge}_{0.98}\text{Mn}_{0.02}$ alloy deposited on Si(001) at 400 °C. The image reveals the co-existence of two kinds of islands: hut islands and dome-shaped islands. The hut islands have a high density and are similar to those previously reported in the case of pure Ge on Si [29, 30]. However, in that case only hut islands were observed at a growth temperature of about 450 °C and dome-shaped islands were observed only when the growth temperature is above 600 °C. Thus, adding a small amount of Mn during Ge deposition on Si has greatly modified the diffusion length of Ge adatoms on the surface and consequently, modified the size and the shape of islands. The dome-shaped islands exhibit two kinds of size: superdomes and flat domes, which are similar to the growth of the $\text{Ge}_{0.98}\text{Mn}_{0.02}$ alloy carried out at 450 °C [37]. Superdomes have a large diameter and an average height of $\sim 12\text{nm}$ (profile 1 in Fig. 2(c)) whereas flat domes have a smaller average height of $\sim 7\text{nm}$ (profile 2 in Fig. 2(c)). To summarize, compared to the case of the growth of pure

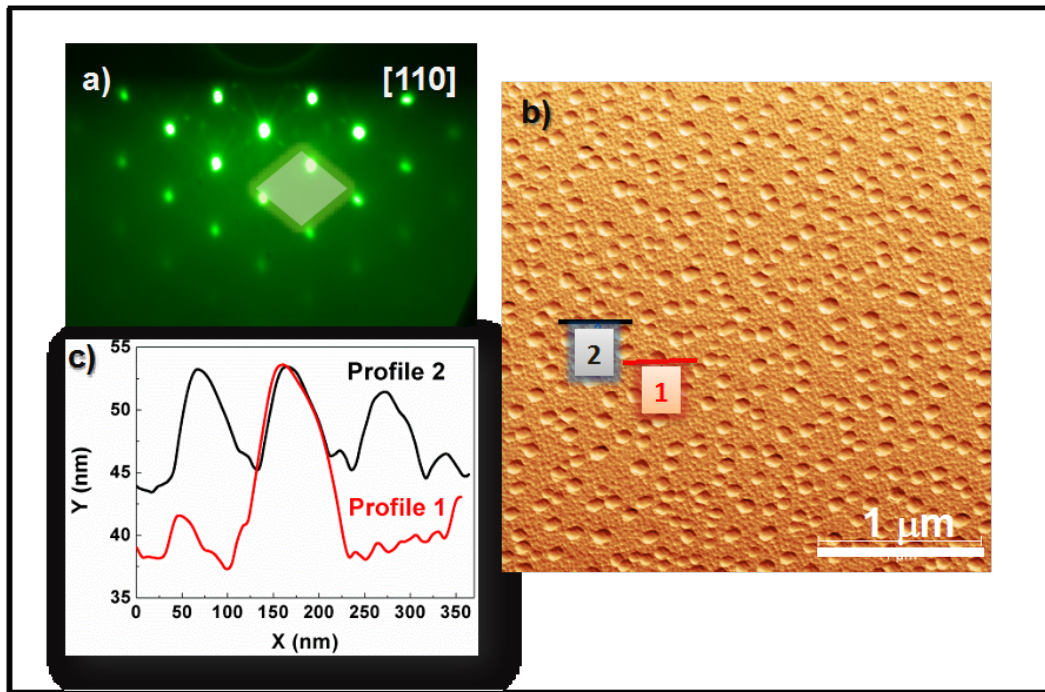


Fig. 2. (a) Typical spotty RHEED pattern characteristic of an island surface. The lozenge represents a unit cell of the GeMn (001) lattice; (b) AFM image showing various types of islands on the surface; (c) AFM profiles of flat domed and super-domed islands.

Ge on Si substrates, the above RHEED diffraction and AFM analyses indicate that incorporation of 2 % of Mn in Ge does not affect the Stranski-Krastanov growth mode but induces a change of the island morphology

Cross-sectional TEM characterizations were systematically performed in order to get an insight into the structural properties of Mn-doped Ge islands. Fig. 3 shows a high-resolution TEM image of a superdomed island, *i.e.* large islands. The image clearly reveals an atomically resolved island and the atomic planes are well continuous from the substrate to the island. This indicates that the island is perfectly epitaxial with the Si substrate. No Mn-rich phases or clusters are visible inside island. Furthermore, using the Fourier transformation (displayed in the inset), we found a diamond cubic lattice of the island, which is as the same as that of the Si(001) substrate. This confirms a high coherence of the island lattice with that of the Si substrate. However, the most important feature revealed from this TEM image is that in contrast to the TEM images shown in Fig. 1 of ref. [36] and Fig. 2 of ref. [37], we do not observe here a buried Mn-rich region that is located just below the island. This implies that for a QD growth at 400 °C, *i.e.* only 50 °C below the temperature used in previous works, the Mn diffusion into the Si substrate has been greatly limited.

To check the Mn presence inside the island and also the Mn diffusion into the substrate region close to the island, we have undertaken chemical composition analysis by means of EDX

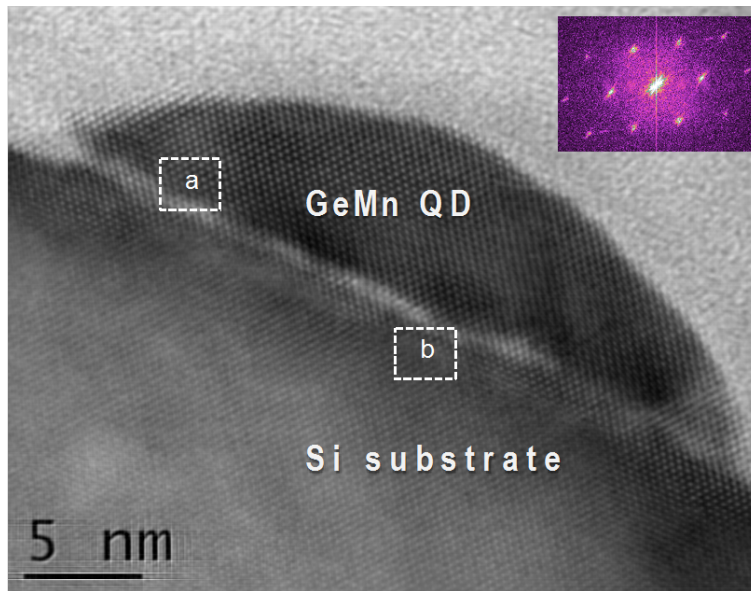


Fig. 3. Cross-sectional TEM image of an atomically resolved superdomed island. Shown in the inset is a Fourier transformation exhibiting a diamond cubic lattice of the quantum dot.

spectroscopy. To get a better resolution from EDX measurements, EDX spectra were sequentially recorded by gently shifting the sample and stabilizing it before each data run.

Figure 4 depicts typical EDX spectra measured in these two regions close to the interface (as indicated by dotted lines in Fig. 3): region (a) is taken inside the island and region (b) in the substrate. It can be clearly seen that both Mn and Ge signals are present in the island region [Fig. 4(a)] while they are completely absent in the substrate region [Fig. 4(b)]. Thus, these measurements confirm the above TEM results on a neglected Mn diffusion into the Si substrate during QD growth. This feature is completely different to the QD formation reported in Refs [36, 37] where important Mn diffusion from QDs to the substrate was observed. We note that the presence of Cu signals in both spectra probably arises from Cu contamination during sample thinning processes for TEM and EDX analysis and the Si signals should come from the substrate as the probed regions are close to the interface.

Figure 5(a) shows the evolution of magnetization as a function of the temperature of the corresponding $\text{Ge}_{0.98}\text{Mn}_{0.02}$ quantum-dot sample. In contrast to the results reported in ref. [37], the magnetization of our sample persists to a temperature higher than 320 K, which is the highest temperature that can be measured in our SQUID system. The hysteresis loops of the corresponding sample, measured at 300 K, is displayed in Fig. 5(b), which clearly confirms the room-temperature ferromagnetic character of $\text{Ge}_{0.98}\text{Mn}_{0.02}$ quantum dots. It is worth noting that for the same Mn concentration of 2 %, the $\text{Ge}_{0.98}\text{Mn}_{0.02}$ thin films, which can be obtained by a growth on a Ge substrate only exhibit a Curie temperature of about 80 K [3, 38]. Thus, the high magnetic ordering observed in $\text{Ge}_{0.98}\text{Mn}_{0.02}$ quantum dots can be explained due to the quantum effect of both carriers and spin inside quantum dots. Another possible explanation is that when the material dimension

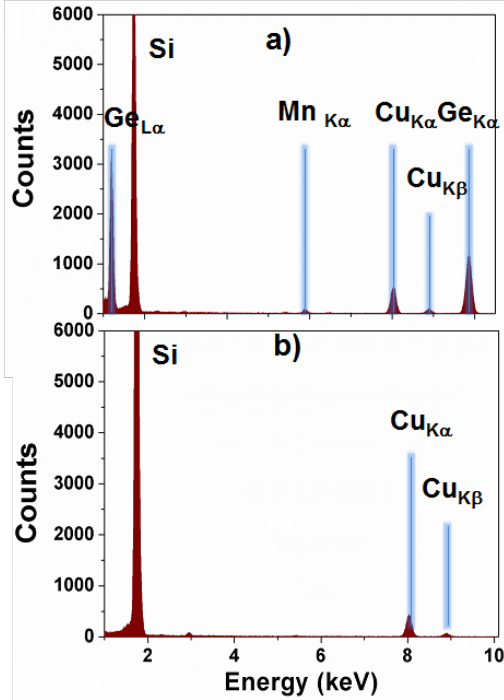


Fig. 4. EDX spectra showing Mn and Ge signatures: (a) within the island and (b) in the substrate region close to the interface.

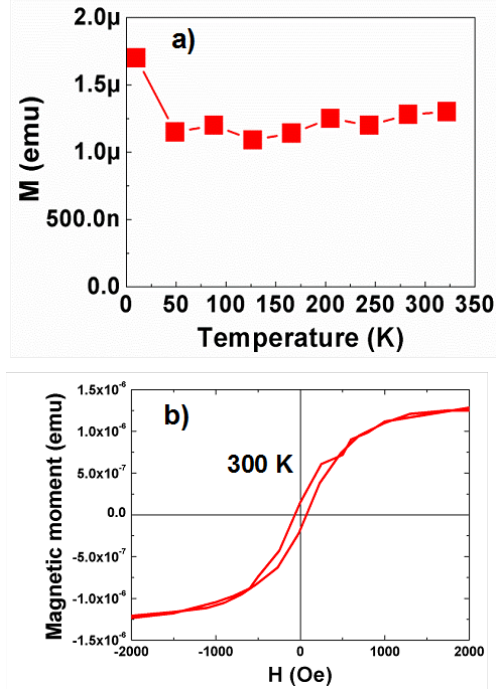


Fig. 5. (a) Evolution of temperature-dependent magnetization at saturation measured with a magnetic field applied parallel to the surface plane. (b) Hysteresis loops measured at 300 K with parallel magnetic field, indicating the ferromagnetic behaviour of the QDs sample.

is reduced down to a size of 30 – 40 nm as in the present case, each quantum dot may behave as a mono-magnetic domain, which allows enhancing the collective magnetic properties of the material

IV. CONCLUSION

To conclude, we have succeeded to grow diluted magnetic Ge_{0.98}Mn_{0.02} quantum dots on a Si(001) substrate using the strain-driven growth mode transition from a two-dimensional growth to a three-dimensional island formation. The quantum-dot formation can be obtained at a substrate temperature as low as 400 °C. Consequently, such a low growth temperature has allowed to greatly reduce both the Mn diffusion into the Si substrate and Ge/Si intermixing. We have also shown that Ge_{0.98}Mn_{0.02} quantum dots are a solid-solution phase without any formation of Mn clusters or Mn-rich phases. The quantum dots are epitaxial and perfectly coherent to the Si substrate. Of great importance, Ge_{0.98}Mn_{0.02} quantum dots exhibit a Curie temperature well above 320 K. It is believed that such high magnetic ordering quantum dots open new perspectives for room-temperature spintronic applications.

ACKNOWLEDGMENTS

This work has been carried out in the frame of a bilateral collaboration agreement signed between the Hong Duc University and the Aix-Marseille University (AMU). We thank Prof. V. Le Thanh and Dr. M.T. Dau at the AMU for their support to this work.

REFERENCES

- [1] The International Technology Roadmap for Semiconductors, , *Emerging Research Materials*, 2009 Edition.
- [2] G. Scappucci, G. Capellini, B. Johnston, W. M. Klesse, J. A. Miwa, and M. Y. Simmons, *Nano Lett.* **11** (2011) 22721.
- [3] Y. D. Park, A. T. Hanbicki, S. C. Erwin, C. S. Hellberg, J. M. Sullivan, J. E. Mattson, T. F. Ambrose, A. Wilson, G. Spanos, and B. J. Jonker, *Science* **295** (2002) 651.
- [4] N. Pinto, L. Morresi, M. Ficcadenti, R. Murri, F. D’Orazio, F. Lucari, L. Boarino, and G. Amato, *Phys. Rev. B* **72** (2005) 165203.
- [5] A. P. Li, J. F. Wendelken, L. C. Feldman, J. R. Thompson, and H. H. Weitering, *Appl. Phys. Lett.* **86** (2005) 152507.
- [6] F. Tsui, L. He, L. Ma, A. Tkachuk, Y. S. Chu, K. Nakajima, and T. Chikyow, *Phys. Rev. Lett.* **91** (2003) 177203.
- [7] C. Bihler, C. Jaeger, T. Vallaitis, M. Gjukic, M. S. Brandt, E. Pippel, J. Woltersdorf, and U. Gosele, *Appl. Phys. Lett.* **88** (2006) 112506.
- [8] L. Morresi, J. Ayoub, N. Pinto, M. Ficcadenti, R. Murri, A. Ronda, and I. Berbezier, *Mater. Sci. Semicond. Process.* **9** (2006) 836.
- [9] M. Passacantando, L. Ottaviano, F. D’Orazio, F. Lucari, M. D. De Biase, G. Impellizzeri, and F. Priolo, *Phys. Rev. B* **73** (2006) 195207.
- [10] S. Ahlers, D. Bougeard, N. Sircar, G. Abstreiter, A. Trampert, M. Opel, and R. Gross, *Phys. Rev. B* **74** (2006) 214411.
- [11] T. Devillers, M. Jamet, A. Barski, V. Poydenot, P. Bayle-Guillemaud, E. Bellet-Amalric, S. Cherifi, and J. Cibert, *Phys. Rev. B* **76** (2007) 205306.
- [12] D. Bougeard, N. Sircar, S. Ahlers, V. Lang, G. Abstreiter, A. Trampert, J. M. LeBeau, S. Stemmer, D. W. Saxe, and A. Cerezo, *Nano Lett.* **9** (2009) 3743.
- [13] Y.D. Park, A. Wilson, A.T. Hanbicki, J.E. Matteson, T. Ambrose, G. Spanos, B.T. Jonker, *Appl. Phys. Lett.* **78** (2001) 2739.
- [14] S. Cho, S. Choi, S.C. Hong, Y. Kim, J.B. Ketterson, B.-J. Kim, Y.C. Kim, J.-H. Jung, *Phys. Rev. B* **66** (2002) 033303.
- [15] A.P. Li, J.F. Wendelken, J. Shen, L.C. Feldman, J.R. Thompson, H.H. Weitering, *Phys. Rev. B* **72** (2005) 195205.
- [16] L. Ottaviano, M. Passacantando, S. Picozzi, A. Continenza, R. Gunnella, A. Verna, G. Impellizzeri, F. Priolo, *Appl. Phys. Lett.* **88** (2006) 061907.
- [17] M. Passacantando, L. Ottaviano, F. D’Orazio, F. Lucari, M. De Biase, G. Impellizzeri, F. Priolo, *Phys. Rev. B* **73** (2006) 195207.
- [18] A. Verna, L. Ottaviano, M. Passacantando, S. Santucci, P. Picozzi, F. D’Orazio, F. Lucari, M. De Biase, R. Gunnella, M. Berti, A. Gasparotto, G. Impellizzeri, F. Priolo, *Phys. Rev. B* **74** (2006) 085204.
- [19] C. Zeng, S. C. Erwin, L. C. Feldman, A. P. Li, R. Jin, Y. Song, J. R. Thompson, and H. H. Weitering, *Appl. Phys. Lett.* **83** (2002) 5002.
- [20] S. Olive-Mendez, A. Spiesser, L. A. Michez, V. Le Thanh, A. Glachant, J. Derrien, T. Devillers, A. Barski, and M. Jamet, *Thin Solid Films* **517** (2008) 191.
- [21] M. Gajdzik, C. Surgers, M. T. Kelemen, and H. V. Lohneysen, *J. Magn. Magn. Mater.* **221** (2000) 248.
- [22] A. Spiesser, I. Slipukhina, M.-T. Dau, E. Arras, V. Le Thanh, L. Michez, P. Pochet, H. Saito, S. Yuasa, M. Jamet, J. Derrien, *Phys. Rev. B* **84** (2001) 165203.
- [23] A. Spiesser, V. Le Thanh, S. Bertaina, L.A. Michez, *Appl. Phys. Lett.* **99** (2011) 121904.
- [24] M.T. Dau, V. Le Thanh, T.G. Le, A. Spiesser, M. Petit, L.A. Michez, R. Daineche, *Appl. Phys. Lett.* **99** (2011) 151908.

- [25] M. T. Dau, V. Le Thanh, L. A. Michez, M. Petit, T. G. Le, O. Abbès, A. Spiesser, and A. Ranguis, *New J. Phys.* **14** (2012) 103020.
- [26] O. Abbès, A. Portavoce, V. Le Thanh, C. Girardeaux, L. Michez, *Appl. Phys. Lett.* **103** (2013) 172405.
- [27] V. Le Thanh, A. Spiesser, M.T. Dau, S.F. Olive-mendez, L. A Michez, M. Petit, *Advances in Natural Sciences : Nanoscience and Nanotechnology* **4** (2013) 043002
- [28] D.J. Eaglesham, M. Cerullo, *Phys. Rev. Lett.* **64** (1990) 1943.
- [29] Y.-W. Mo, D.E. Savage, B.S. Swartzentruber, M.G. Lagally, *Phys. Rev. Lett.* **65** (1990) 1020.
- [30] V. Le Thanh, *Surf. Sci.* **492** (2001) 255
- [31] V. Le Thanh, P. Boucaud, D. Débarre, Y. Zheng, D. Bouchier, and J. M. Lourtioz, *Phys. Rev. B* **58** (1998) 13115
- [32] G. Medeiros-Ribeiro, A. M. Bratkovski, T. I. Kamins, D. A. A. Ohlberg, and R. S. Williams, *Science* **279** (1998) 353
- [33] A. V. Baranov, A. V. Fedorov, T. S. Perova, R. A. Moore, V. Yam, D. Bouchier, V. Le Thanh, K. Berwick, *Phys. Rev. B* **73** (2006) 075322
- [34] U. Denker, M. Stoffel, and O. G. Schmidt, *Phys. Rev. Lett.* **90** (2003)196102
- [35] T.K.P. Luong, M.T. Dau, M.A. Zrir, M. Stoffel, V. Le Thanh, M. Petit, A. Ghrib, M. El Kurdi, P. Boucaud, H. Rinnert, J. Murota, *J. Appl. Phys.* **114** (2013) 083504.
- [36] F. Xiu, Y. Wang, J. Kim, A. Hong, J. Tang, A. P. Jacob, J. Zou, and K. L. Wang, *Nat. Mater.* **9** (2010) 337
- [37] J. Kassim, C. Nolph, M. Jamet, P. Reinke, and J. Floro, *Appl. Phys. Lett.* **101** (2012) 242407
- [38] T. G. Le, D. N. H. Nam, M. T. Dau, T. K. P. Luong, N. V. Khiem, V. Le Thanh, L. Michez, and J. Derrien, *J. Phys.: Conf. Ser.* **292** (2011) 012012